Admissible Blowdown Loading for Spherical Containments with Pressure Suppression System

R. Krieg, B. Göller, G. Hailfinger
Institut für Reaktorentwicklung,
Kernforschungszentrum Karlsruhe GmbH,
Postfach 3640, D-7500 Karlsruhe, Germany

Containments of boiling water reactors usually are equipped with a so-called pressure suppression system. It consists of a condensation chamber which contains a large water pool. In case of a postulated failure of the primary system the escaping steam will be blown through condensation tubes into this water pool and condensed.

The condensation process, however, may be very transient. Inside the water pool at the muzzles of the condensation tubes the steam volume grows relatively slowly and then collapses in time of some ten milliseconds. As a consequence, pressure transients in the water pool and oscillations of the walls of the condensation chamber are generated.

In this paper the oscillations of German pressure suppression systems type 69 are investigated where the condensation chamber is located inside the spherical containment. Therefore, the pressure transients and oscillations affect directly the containment structure.

The calculations show that consideration of the fluid inertia of the water pool reduces the eigenfrequencies significantly and increases the transient pressure loading. Without fluid inertia the smallest shell eigenfrequency is about 50 Hz. Including fluid inertia the smallest eigenfrequency is now in the order of 10 Hz, but the maximum pressure loading is about 40 % higher than before.

Strong stress gradients occur in the spherical containment close to the intersection with the bottom of the water pool. Therefore, high spatial resolution is required.

Final results are presented in terms of admissible steam condensation scenarios where the stress reach their allowed upper limit. If these admissible scenarios cover all steam condensation events which may occur, the dimensions of the containment shell are adequate to blowdown loading. In this way the complex physics of steam condensation which has a certain statistical character and requires extensive experimental investigations is clearly distinguished from the fluid-structure interaction and shell dynamics problem which can be investigated on a mathematical basis.

1. Introduction

The dynamic behaviour of pressure suppression systems during steam condensation and the consequences on nuclear reactor safety have been investigated in many publications. Examples are the refs [1-5]. Depending on the particular designs different physical effects have been in view and different analysis methods have been applied.

This paper concentrates on the German pressure suppression system type 69, which is located inside the spherical containment. A typical example is shown in fig. 1. The outer wall of the condensation chamber is part of this containment. In case of a postulated failure of the primary system the escaping steam is blown into the condensation chamber. Here the steam is condensed. Thus the containment pressure can be kept at a rather low level.

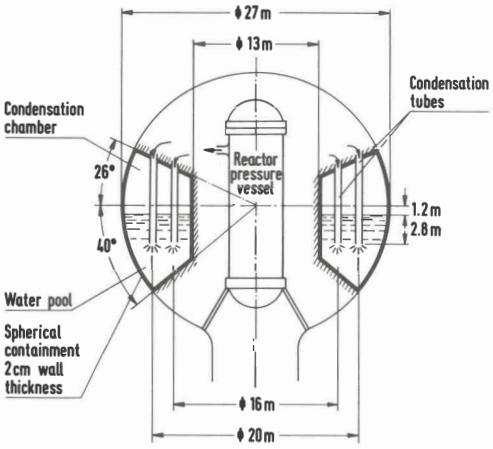

Fig. 1: Containment of boiling water reactor with pressure suppression system German type 69

However, during the condensation process highly transient loadings may occur. At the beginning large amounts of air are blown into the water pool. As a consequence, the free water surface moves upward and may hit structural elements. This phenomenon is known under term pool swelling.

It should be mentioned, however, that for the type 69 sensitive structural elements like large horizontal steam tubes (headers) do not exist in the upper part of the condensation chamber. In this paper pool swelling is not investigated.

Later the amount of air fed into the pressure suppression system decreases. Then the pool dynamics is controlled by the steam condensation which may have a very instable character. For relative small flow rates with the condensation occurring inside the blowdown tubes, water is periodically ejected into the pool. For high flow rates large steam bubbles may be formed outside of the blowdown tubes. Due to instability effects these bubbles collapse in times of some ten milliseconds. Both phenomena are known under the term chugging.

These phenomena may cause strong pressure pulses in the water pool and significant dynamic responses of the surrounding structures. In this paper these consequences will be investigated. A more detailed description of this work may be found in [6].

2. Steam Condensation

The process of steam condensation is governed by several competitive effects like rate of steam supply, turbulences in steam and water, heat conduction, and surface tension, for instance. Small parameter changes have strong influences on the results. Therefore, a deterministic steam condensation model can hardly be more than a very rough description. As a further consequence, the development of a steam condensation model based on first principles

is practically impossible. The inevitable uncertainties of the particular parameters would lead to extreme uncertainties of the results.

Therefore, in this paper the steam condensation model is primarily based on experimental observations and some additional theoretical assessments. Following a proposal of Class [7] the steam condensation is modelled as a transient point source located at the muzzles of the condensation tubes. The time history of the volume V fed into the water pool is qualitatively shown in fig. 2. The time t_p denotes one condensation period. During this time the volume grows rather slowly from zero to the maximum V_o. Then it collapses very rapidly within the time t_o:

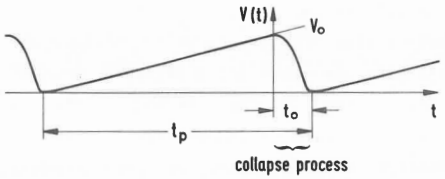

Fig. 2: Volume expansion due to a point source simulating steam condensation

$$V(t) = V_o \left[1-(t/t_o)^4\right]^3, \qquad 0 \le t \le t_o. \tag{2.1}$$

Typical values are

$$t_p \approx 1 \div 2 \text{ s}, \quad t_o \approx 0.02 \div 0.1 \text{ s}.$$

According to the high parameter sensitivity of the steam condensation process, certain stochastic effects are inevitable. Therefore, the time history in fig. 2 is not exactly periodic. Rather the collapses occur within so-called time windows [7].

For the dynamic excitation of the system only the relative quick collapse process is important. Consequently, the interaction between steam condensation and the fluid dynamics of the water pool will be described by eq. (2.1) only.

Possible feedbacks from the fluid dynamics on the thermodynamics of transient steam condensation are neglected in this equation. Some additional investigations of this problem have been published by Antony-Spies [8]. His results show a certain influence of the water pool geometry on the bubble eigenfrequencies. In addition, there are hints that the feedback on the thermodynamics also controls the collapse initiation within the time window mentioned above. However, the influence on the expansion volume V_o and the collapse time t_o is expected to be rather low.

Therefore, these values may be determined by condensation experiments where only one tube is blowing into a relatively small water pool representing only a corresponding part of the pressure suppression system. A detailed modelling of the geometry of the water pool and geometry and flexibilities of the surrounding structures is not necessary. In other words, for investigation of steam condensation expensive experiments in a full scale mock-up of a pressure suppression system are not necessary.

Nevertheless, the determination of the expansion volume V_o and the collapse time t_o by evaluation of experiments represents a problem. According to the high parameter sensitivity of the steam condensation process the values obtained spread over wide ranges. Therefore, the definition of most unfavorable values which must be used for stress analysis is a difficult task. It should be done by steam condensation experts, who also have in mind the load carrying capacity of the structure.

Therefore, in this paper relevant values for V_o and t_o have not been defined and resulting stresses have not been calculated. Rather the allowed stresses have been used as a basis. Then admissible steam condensation scenarios including admissible values for V_o and t_o have been determined such that the allowed stresses are almost reached. However, a detailed comparison with the experimental findings and an assessment of the remaining safety margins is not included.

3. Fluid Dynamics of the Water Pool

The fluid dynamics of the water pool is important in order to describe the transfer of mechanical energy from the steam condensation to the surrounding shells.

From some rough estimates it follows that relevant times for the dynamic behaviour of these shells are between 20 and 100 ms. On the other hand the times for a pressure wave to traverse characteristic regions of the water pool are in order of only 5 ms and may thus be neglected. Therefore, the fluid in the water pool can be treated as incompressible. This conclusion has been confirmed using a simplified theoretical model where the fluid compressibility could be varied [9].

In comparison with most classical flow problems the velocities in the water pool are very small except the close regions of steam condensation. Therefore, the fluid in the water pool can be treated as inviscid. Furthermore, the so-called dynamic pressures, defined as half the fluid density times the square of the fluid velocity, are small, too. Therefore, at the fluid boundaries these terms can be neglected. Furthermore, the displacements of the fluid boundaries can be assumed to be small in comparison with the water pool dimensions.

Under these conditions the field equations for the transient fluid dynamics of the water pool read:

$$\operatorname{div} \bar{a} = 0 \text{ (continuity)}, \qquad \bar{a} + \frac{1}{\rho} \operatorname{grad} p = 0 \text{ (momentum)}, \tag{3.1}$$

where $\bar{a}$ is the acceleration vector, p is the total transient pressure (pressure head), and ρ is the fluid density.

The boundary conditions require that

- at the flexible containment shell the pressure p and the normal component of the acceleration vector $\bar{a}$ must agree with the corresponding quantities describing the structural dynamics of these walls;
- at rigid walls the normal components of the acceleration vector $\bar{a}$ must vanish;
- at the free surface of the pool the pressure p must assume prescribed values.

At the muzzles of the condensation tubes point sources are defined according to eq. (2.1). The geometry of the condensation tubes is not taken into account, i.e., the tube walls are not treated as fluid boundaries.

Since the description of the transient fluid dynamics constitutes linear relationships between pressures and accelerations, the principle of superposition applies. Therefore, the advanced boundary integral equation method described in refs. [10, 11] can be used for solution. With this method the pool boundary is approximately formed by plane rectangular panels as shown in fig. 3. At the midpoints of these panels the boundary conditions will be satisfied.

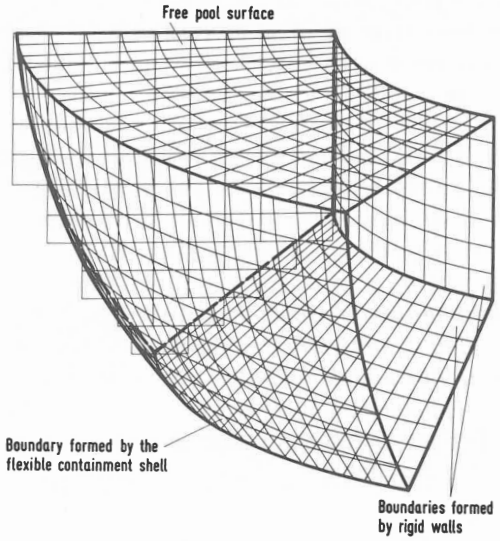

Fig. 3: Panel discretization of a 60°-section of the water pool

This leads to the following equation:

$$\bar{a}^{1} - \bar{\bar{F}}\bar{p}^{1} = \bar{q}^{1x}. \qquad (3.2)$$

The components of the vector $\bar{a}^{1}$ are the normal accelerations and the components of the vector $\bar{p}^{1}$ are the pressures of those panels describing fluid boundaries which are formed by flexible shells. The elements of the matrix $\bar{\bar{F}}$ can be calculated using the pool dimensions. The vector $\bar{q}^{1x}$ depends on the prescribed sources at the mozzles of the condensation tubes. This means, eq. (3.2) constitutes a linear relationship between unknown accelerations and pressures of the fluid boundary.

A unique determination of these unknowns $\bar{a}^{1}$ and $\bar{p}^{1}$ is not possible on the basis of eq. (3.2), i.e. a unique solution of the flow problem in the water pool is not possible on the basis of the fluid dynamics relations alone. Rather information about the flexibilities of the shells forming the fluid boundaries is necessary, i.e., one has to deal with a problem in fluid-structure interaction.

4. Structural Dynamics of the Spherical Containment

The most crucial wall of the condensation chamber is that formed by the spherical containment shell. It must carry both, the pressure pulses from steam condensation and the quasi-static pressure increase in the containment. Therefore, stresses will be calculated only for this part of the containment.

The influence of the flexibility of other parts of the spherical containment can be assumed to be small. This is shown in [6, 9, 12, 13] where the local displacements of thin spherical shells were found to be almost proportional to the corresponding local pressure. The influence of the flexibility of other walls of the condensation chamber are also assumed to be small. Most of these walls are stiffened by additional ribs. Consequently structural flexibilities will be considered only for the spherical wall of the condensation chamber.

According to the safety requirements the stresses must not reach the yield point. Therefore the equation of motion of the spherical wall of the condensation chamber can be put in the following linear form:

$$\bar{\bar{A}}^{11}\bar{s}^{1} + \bar{\bar{A}}^{12}\bar{s}^{2} + \bar{\bar{B}}^{11}\ddot{\bar{s}}^{1} + \bar{\bar{B}}^{12}\ddot{\bar{s}}^{2} = \bar{q}^{1}, \quad \bar{\bar{A}}^{21}\bar{s}^{1} + \bar{\bar{A}}^{22}\bar{s}^{2} + \bar{\bar{B}}^{21}\ddot{\bar{s}}^{1} + \bar{\bar{B}}^{22}\ddot{\bar{s}}^{2} = \bar{q}^{2}. \qquad (4.1)$$

The components of the vector $\bar{s}^{1}$ are the normal displacements in structural points at the fluid-structure interaction region. These structural points must be assigned to the midpoints of the panels describing the fluid dynamics of the water pool. The components of the vector

$\underline{q}^1$ are the loads per unit area associated with the displacements of the vector $\underline{s}^1$. The components of the vector $\underline{s}^2$ denote all other displacements which have been introduced for an appropriate description of the shell. The components of the vector $\underline{q}^2$ are the corresponding loads. Usually $\underline{q}^2$ vanishes. The symbol $\ddot{\underline{s}}^1$ and $\ddot{\underline{s}}^2$ denote the second time derivatives of $\underline{s}^1$ and $\underline{s}^2$, respectively.

$\bar{\bar{A}}^{11},\ldots,\bar{\bar{A}}^{22}$ are stiffness matrices, $\bar{\bar{B}}^{11},\ldots,\bar{\bar{B}}^{22}$ are mass matrices which can be calculated on the basis of the given shell dimensions and material properties. However, care should be taken when standard methods are used. In [9] it is shown that an extremely high number of standard finite elements would be required for an appropriate description of the shell dynamics.

In eqs. (4.1) the right hand sides must be known for determination of the unknown displacements $\underline{s}^1$ and $\underline{s}^2$. However, the load $\underline{q}^1$ is not explicitely given. Rather it stems from the fluid pressure $\underline{p}^2$ in the water pool, i.e., fluid-structure interaction must be considered.

5. Fluid-Structure Interaction between Water Pool and Spherical Containment

The basic equations are very simple:

$$\underline{q}^1 = -\underline{p}^1 \qquad \underline{a}^1 = \ddot{\underline{s}}^1 \tag{5.1}$$

The first one requires that the shell loading corresponds with the pressures at the pool boundary and the second one requires that the normal shell displacements correspond with the motions at the pool boundary.

Now with eqs. (5.1) the fluid dynamics relation (3.2) can be used in order to eliminate the unknown load $\underline{q}^1$ in the structural dynamics relation (4.1). This leads to the equation of motion for the fluid-structure interaction problem, describing the dynamics of the water pool coupled with the flexibility of the spherical containment shell:

$$\begin{aligned}
&(\bar{\bar{F}}\bar{\bar{A}}^{11})\underline{s}^1 + (\bar{\bar{F}}\bar{\bar{A}}^{12})\underline{s}^2 + (\bar{\bar{F}}\bar{\bar{B}}^{11} + \bar{\bar{E}})\ddot{\underline{s}}^1 + (\bar{\bar{F}}\bar{\bar{B}}^{12})\ddot{\underline{s}}^2 = \underline{q}^{1*} \\
&\bar{\bar{A}}^{21}\underline{s}^2 + \bar{\bar{A}}^{22}\underline{s}^2 + \bar{\bar{B}}^{21}\ddot{\underline{s}}^2 + \bar{\bar{B}}^{22}\ddot{\underline{s}}^2 = \underline{q}^2
\end{aligned} \tag{5.2}$$

$\bar{\bar{E}}$ is the identity matrix.

Eqs. (5.2) are of the same type as the equations of motion for the structural dynamics. The matrices governing the interaction problem have the same dimensions as the stiffness and mass matrices for the structure. However, now the right hand sides $\underline{q}^{1*}$ and $\underline{q}^2$ are known. Therefore, with initial conditions eqs. (5.2) can be solved for the transient structural displacements $\underline{s}^1$ and $\underline{s}^2$. The methods used may be the same as those applied in structural dynamics.

Once the structural displacements are known, the loading $\underline{q}^1$ may be easily determined using eqs. (4.1).

A more detailed description of the fluid-structure interaction may be found in [6, 14, 15].

6. Results for Displacements and Loadings of the Spherical Containment

In order to carry out the calculations discussed before, the computer code SING-S has been written [10, 11]. The stiffness matrices $\bar{\bar{A}}^{11},\ldots,\bar{\bar{A}}^{22}$ have been obtained based on ana-

lytical solutions of Flügge's shell equatins. The computer code used was SPHERE-DYNA [12, 13]. Both codes have been assessed by application to test problems where experimental data were available [6].

For analysis of the pressure suppression system threefold periodicity around the circumference of the system and symmetry about a meridional plane for each of the resulting 120-degree sections have been assumed. Therefore, only a 60-degree section of the water pool had to be discretized by panels (see fig. 3).

The following cases have been investigated:

Case 1. The whole outer wall of the condensation chamber is assumed to be flexible (shell clampings at $\phi_1 = 26^o$ and $\phi_2 = 40^o$). The fluid inertia is included.

Case 2. The whole outer wall of the condensation chamber, except the three lowest rows of panels is assumed to be flexible (shell clampings at $\phi_1 = 26^o$ and $\phi_2 = 27^o$). The fluid inertia is included.

Case 3. The whole outer wall of the condensation chamber, except the three lowest rows of panels is assumed to be flexible (shell clampings at $\phi_1 = 26^o$ and $\phi_2 = 27^o$). The fluid inertia is included. At the muzzle of one outer condensation tube a not condensing spherical bubble with constant pressure and 0.5 m diameter is assumed.

Case 4. The same as Case 1, however, without fluid in the condensation chamber.

Case 5. The same as Case 2, however, without fluid in the condensation chamber.

In a first step the eigenfrequencies of the system have been calculated. Some of the values obtained are listet in table I. The corresponding deformation modes may be characterized by their axial and circumferential orders. Due to the above assumptions the circumferential orders include only the numbers 0, 3, 6,... More information may be found in [16].

Table I: Eigenfrequencies (Hz)

Fluid-structure Interaction:					
90 degrees of freedom		250 degrees of freedom			
Case 1 	Case 2 	Case 2 	Case 3 	Case 4 	Case 5 
9.36	13.12	12.49	12.62	46.56	51.97
13.01	15.81	14.90	15.03	54.73	56.01
17.52	19.27	17.87	17.90	57.24	58.82
17.81	22.42	20.45	20.40	58.07	59.10
19.31	23.30	21.50	21.51	58.37	59.50
21.44	24.31	22.30	22.31	59.05	60.05
21.92	25.39	22.79	22.79	59.11	60.23
24.40	25.96	23.62	23.62	59.24	60.87
24.77	27.89	24.98	24.98	59.46	60.93
24.96	28.27	25.05	25.05	59.61	61.11
25.06	30.14	26.62	26.62	59.71	61.24
26.46	31.01	27.09	27.09	59.72	61.61

For Case 2 calculations have been done first with 90 and then with 250 degrees of freedom. Consequently, for this case the influence of different computational effort can be studied by comparing column two and three in table I. Furthermore, comparison of Case 1 and 2 shows that stiffening of the containment shell at the three lowest rows of panels increases the eigenfrequencies up to 40 %. Comparison of Case 2 and 3 shows that consideration of a spherical not yet condensing steam bubble at the muzzle of an outer condensation tube increases the eigenfrequencies, too. However, these changes are very small. Finally, Case 4 and 5 are included in order to demonstrate the strong influence of the fluid inertia on the eigenfrequencies.

Based on the eigenfrequencies and the corresponding deformation modes transient

system responses have been calculated. The system excitation was assumed to be caused by steam condensation either at the muzzle of one outer or one inner condensation tube. Due to the postulated threefold periodicity of the problem the same steam condensation is automatically assumed to occur at the angular distances of ± 120°. The time history of steam condensation was modeled according to eq. (2.1) with the collapse times t_o = 0.025, 0.05, 0.08, 0.10 s. The reference value of the maximum volume expansion was assumed to be V_o = 0.523 m^3. It corresponds to sphere with a diameter of 1 m. With known results for this value of V_o the transient system responses due to other values of V_o can easily be determined, since the calculated pressures and displacements are proportional to V_o.

Extensive transient results are presented in [16]. In fig. 4 the maximum radial displacements are plotted versus the collapse time. The cross-sections of the condensation chamber indicate the particular cases; the stars indicate whether the steam condensation occurs at the muzzle of an outer or an inner condensation tube. Comparison between the upper and lower diagram shows that stiffening of the containment shell at the three lowest rows of panels increases the maximum displacements. Furthermore, the maximum displacements increase with reducing collapse time. They are higher for steam condensation at the muzzle of an outer than of an inner condensation tube. In the meridional plane where the steam condensation occurs the maximum displacements are reached within the first or second peak. In a 60° angular distance wave propagation effects cause certain delays. Therefore, the maximum displacements are reached somewhat later after several peaks. Finally, Case 3 shows that the existence of not yet condensing steam bubbles in the water pool considerably reduces the maximum displacements of the containment shell.

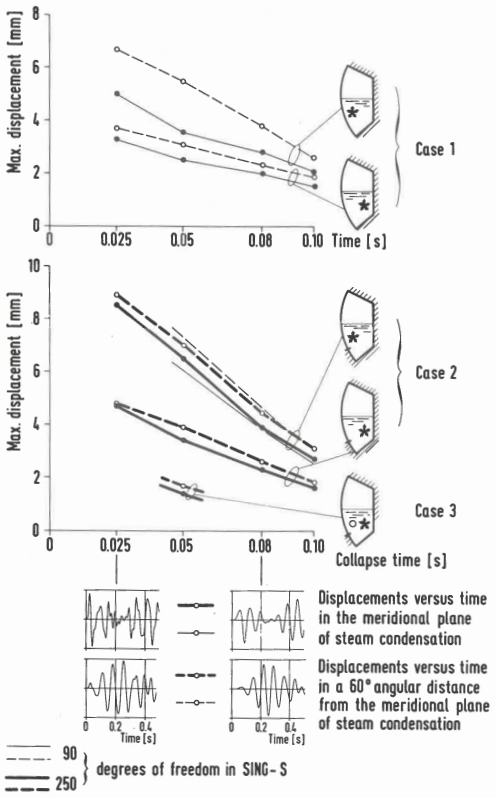

Fig. 4: Maximum radial shell displacement vs. collapse time

Based on the calculated displacements the transient pressure distributions at the spherical wall of the condensation chamber have also been determined. It was found that the local displacements are roughly proportional to be local pressures. The ratio is about 5 mm/bar. This has been predicted as a consequence of the local deformation character of thin spherical shells discussed in [9, 13].

Corresponding pressure distributions have been calculated ignoring the flexibility of the spherical containment, i.e., ignoring the fluid-structure interaction. It was found that considering fluid-structure interaction increases the maximum pressures by about 40 % in comparison with the results without this effect.

This may be explained as follows: In case of a flexible containment shell the maximum pressure consists of the pressure field caused by the prescribed volume source modelling the steam condensation and the pressure field caused by the containment oscillations. The second contribution is proportional to the radial displacements. When the displacements reach their maxima the fluid is decelerated in radial direction generating a corresponding pressure field. This field does not occur in case of a rigid containment.

7. Determination of Admissible Condensation Scenarios

Due to the extremely small wall thickness of the containment in comparison with its radius, high stress gradients are expected close to the intersection with the bottom of the water pool where the containment is assumed to be rigidly clamped. This requires high spatial resolution. Therefore, the stresses in the containment shell are determined on the basis of the calculated pressure distributions using the computer code SPHERE-STRESS. In comparison, stress analysis on the basis of the calculated containment displacements would be simpler but less accurate. An example for the equivalent stress distribution (membran and bending) along a meridian of the spherical wall of the condensation chamber is shown in fig. 5.

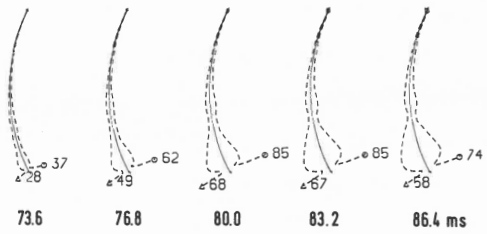

Fig. 5: Equivalent stress (Δ outside, O inside) along a containment meridian for case 2. Steam condensation at three outer tubes, $V_o = 0.523\ m^3$, $t_o = 0.08$ sec.

However, such stress distributions are not given as final results. Rather steam condensation scenarios are determined such that the above stresses superimposed with the membran stresses due to the weight and the global pressure increase inside the containment reach 75 % of yield stress which was assumed to be $370\ N/mm^2$ / 17 /. The results are presented in figs. 6 and 7. Assuming steam condensation according to eq. (2.1), the admissible maximum volume expansion V_o depends on the collapse time t_o. Small values of V_o are obtained for rapid collapses with $t_o = 0.025$ s. Values about three times higher are obtained for slower collapses with $t_o = 0.1$ s.

Furthermore, for steam condensation at the muzzles of inner condensation tubes the admissible values V_o are higher than for outer condensation tubes. For simultaneous condensation at the muzzles of inner and outer condensation tubes the admissible values V_o are described by the lowest curve. Comparison between fig. 6 and 7 shows that the admissible volume expansions at three single outer condensation tubes are about 6 times higher than the values for simultaneous condensations at all condensation tubes. Based on figs. 6 and 7 any superposition of simultaneous condensation at the muzzles of all condensation tubes with larger condensation events at the muzzles of single condensation tubes can be described.

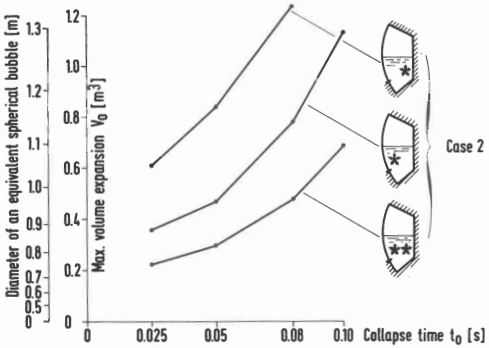

Fig. 6: Admissible maximum volume expansions for simultaneous condensation in three meridional planes

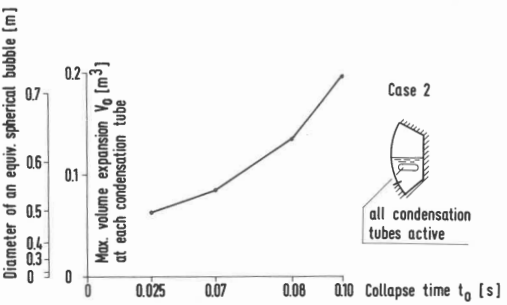

Fig. 7: Admissible maximum volume expansions for simultaneous condensation in all condensation tubes

The results in figs. 6 and 7 do not include the effects of uncondensed steam bubbles or air bubbles in the water pool. However, as shown in fig. 4 the existence of such bubbles reduces the containment response considerably. Consequently with respect to this effect the presented results are conservative.

Literature

[1] Di Maggio, F.L., et al., Computers & Structures 8 (1978) 31-39

[2] Giencke, E., SMIRT-5, Berlin, Aug. 1979, paper B7/1*

[3] Nichols, B.D., and Hirt, C.W., SMIRT-5, Berlin, Aug. 1979, paper B7/2

[4] Norris, D.M, et al., Nucl. Engrg. Des. 59 (1980) 301-313

[5] McMaster, W.H., et al., Lawrence Livermore Lab., NUREG/CR-1179, UCRL-52733 (1979)

[6] Krieg, R., Göller, B., and Hailfinger, G., Nucl. Engrg. Des. 64 (1981)

[7] Class, G., Kernforschungszentrum Karlsruhe, KfK 2487 (1977)

[8] Antony-Spies, P., SMIRT-5, Berlin, Aug. 1979, paper B7/3

[9] Göller, B., Kernforschungszentrum Karlsruhe, KfK 2778 (1979)

[10] Krieg, R., Göller, B., and Hailfinger, G., Comput. Physics 34(2) (1980) 139-183

[11] Krieg, R., and Hailfinger, G., SMIRT-5, Berlin, Aug. 1979, paper B8/2*

[12] Göller, B., SMIRT-5, Berlin, Aug. 1979, paper B8/3

[13] Göller, B., J. Sound and Vibration 73(4) (1980) 585-596

[14] Krieg, R., Appl. Math. Modelling 2 (1978) 81-89

[15] Krieg, R., Göller, B., and Hailfinger, G., SMIRT-5, Berlin, Aug. 1979, paper B8/4

[16] Hailfinger, G., and Krieg, R., Kernforschungszentrum Karlsruhe, KfK 2779B (1979)

[17] Sicherheitstechnische Regel des KTA, Reaktorsicherheitsbehälter aus Stahl, Teil: Auslegung, Konstruktion und Berechnung KTA 3401.2, Carl Heymanns Verlag, Köln, 1979